

## Nanosized Hybrid Oligoamide Foldamers: Aromatic Templates for the Folding of Multiple Aliphatic Units

David Sánchez-García,<sup>†,‡</sup> Brice Kauffmann,<sup>†</sup> Takahiro Kawanami,<sup>‡</sup> Hirotaka Ihara,<sup>‡</sup> Makoto Takafuji,<sup>‡</sup> Marie-Hélène Delville,<sup>§</sup> and Ivan Huc<sup>\*,†</sup>

*Institut Européen de Chimie et Biologie, Université de Bordeaux—CNRS UMR5248 and UMS3033, 2 rue Robert Escarpit, 33607 Pessac, France, Department of Applied Chemistry and Biochemistry, Kumamoto University, 2-39-1 Kurokami, Kumamoto 860-8555, Japan, and Institut de Chimie de la Matière Condensée de Bordeaux, CNRS UPR9048, 87 avenue du Dr Albert Schweitzer, 33608 Pessac, France*

Received March 13, 2009; E-mail: i.huc@iecb.u-bordeaux.fr

**Abstract:** Oligoamide sequences comprised of both 8-amino-2-quinolinecarboxylic acid “Q” and 6-aminomethyl-2-pyridinecarboxylic acid “P” have been synthesized. It was found that the aliphatic amine of P greatly facilitates amide couplings, as opposed to the aromatic amine of Q, which enabled us to prepare sequences having up to 40 units. The conformation and conformational stability of these oligomers were characterized in the solid state using X-ray crystallography and in solution using NMR and various chromatographic techniques. Q<sub>n</sub> oligomers adopt very stable helically folded conformations whereas P<sub>n</sub> oligomers do not fold and impart conformational preferences distinct from those of Q units. When a P<sub>n</sub> segment is attached at the end of a Q<sub>4</sub> segment, a couple P units appear to follow the folding pattern imposed by the Q<sub>n</sub> segment, but P units remote from the Q<sub>n</sub> segment do not fold. When a P<sub>n</sub> segment is inserted between two Q<sub>4</sub> segments, the P<sub>n</sub> segment adopts the canonical helical conformation imposed by the Q units at least up to two full helical turns ( $n = 5$ ). However, the overall stability of the helix tends to decrease as the number of P units increases. When noncontiguous P units separated by Q<sub>4</sub> segments are incorporated in a sequence, they all adopt the helical conformation imposed by Q monomers and the overall helix stability increases when helix length increases. For example, a 40mer with a sequence (PQ<sub>4</sub>)<sub>8</sub> folds into a rod-like helix spanning over 16 turns with a length of 5.6 nm. This investigation thus demonstrates that remarkably long (nanometers) yet well-defined foldamers can be efficiently synthesized stepwise and that their helical stability may be continuously tuned upon controlling the ratio and sequence of P and Q monomers.

### Introduction

Biopolymers' extraordinary functions are based on their exquisite ability to adopt well-defined folded conformations. From the perspective of organic chemistry, it is striking that biopolymers achieve such a wide range of structures and functions from relatively small sets of monomeric units and their arrangement into well-ordered sequences: four nucleobases for nucleic acids and 20 amino acids for proteins. These basic facts have led to considerable interest in folding phenomena at large and in the prospect of eliciting the structural patterns of biopolymers in non-natural scaffolds. In this context, a diverse range of chemically synthesized foldamers have been prepared and shown to adopt folded conformations mimicking the secondary structural elements of proteins and polynucleotides such as helices, turns, and linear strands.<sup>1</sup> Mimics of supersecondary, tertiary, and quaternary structures have also begun to appear.<sup>2</sup>

A fundamental feature of proteins and nucleic acids is that they consist of variable side chains but of a constant repeat unit in their main chain due to the enzyme-controlled polymerization processes on which Nature relies to produce them. Most synthetic foldamer families also consist of a constant main chain and variable side chains.<sup>1</sup> In those cases, the side chains are often critical to determine the folded conformation of the main chain, either directly because they impart local constraints on the main backbone or indirectly because side chains engage in intra or intermolecular interactions. An example of the former is the propensity of Asn-Gly to adopt a turn structure in  $\alpha$ -peptides.<sup>3</sup> Examples of the latter include cross-strand interactions in  $\beta$  sheet or helix-loop-helix peptidic structures,<sup>4</sup> various types of base-pairing in nucleic acids giving rise to duplex,

- (1) For recent reviews, see: (a) Li, Z.-T.; Hou, J.-L.; Li, C. *Acc. Chem. Res.* **2008**, *41*, 1343–1353. (b) Seebach, D.; Gardiner, G. *Acc. Chem. Res.* **2008**, *41*, 1366–1375. (c) Gong, B. *Acc. Chem. Res.* **2008**, *41*, 1376–1386. (d) *Foldamers: Structure, Properties and Applications*; Hecht, S. M., Huc, I., Eds.; Wiley-VCH: Weinheim, Germany, 2007. (e) Goodman, C. M.; Choi, S.; Shandler, S.; DeGrado, W. F. *Nat. Chem. Biol.* **2007**, *3*, 252–262. (f) Li, Z.-T.; Hou, J.-L.; Li, C.; Yi, H.-P. *Chem. Asian J.* **2006**, *1*, 766–778. (g) Huc, I. *Eur. J. Org. Chem.* **2004**, 17–29.

<sup>†</sup> Université de Bordeaux.

<sup>‡</sup> Kumamoto University.

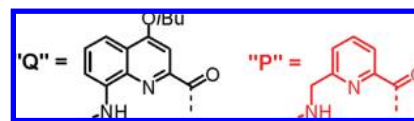
<sup>§</sup> CNRS UPR 9048.

<sup>\*</sup> Current address: Institut Químic de Sarrià, Universitat Ramon Llull, Via Augusta 390, 08017 Barcelona, Spain.

triplex, or quadruplex structures,<sup>5</sup> or interstrand side chain interactions in some foldamers.<sup>6</sup>

Chemical synthesis, however, does not only give access to structural and functional patterns that Nature uses but also to structures and functions that Nature does not use. Along this line, recent investigations in foldamer research focused on sequences where not only side chains but also main chain components can be varied. Such sequences may consist of two or more kinds of monomers assembled in a regular repeat motif or not. Thus  $\alpha$ ,  $\beta$ , and  $\gamma$  aliphatic peptides have been assembled into various combinations.<sup>2e,7</sup> Aromatic amide monomers of various sizes and shapes have been combined as well.<sup>2b,8,9</sup> In recent years, several foldamers possessing hybrid aromatic–aliphatic

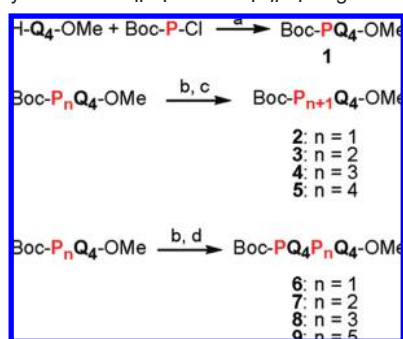
Chart 1



backbones have also been described.<sup>10–14</sup> A remarkable aspect of these aromatic and aliphatic-aromatic hybrid sequences is that, unlike foldamers that consist of a constant backbone repeat, they often give rise to folded patterns that have no counterparts in biopolymer structures. For instance, helices whose diameter varies along the sequence,<sup>8</sup> helices possessing a handedness inversion center,<sup>2b</sup> knots,<sup>11</sup> “tail biters”,<sup>13</sup> pillars,<sup>10</sup> and heringbone helices<sup>14</sup> have been reported.

In this work, we explore the extent to which two non natural monomers having profoundly different folding propensities can be combined in such a way that a “dominant” monomer imparts its properties to a “recessive” monomer and eventually templates the folding of very large architectures comprised of both units. The two monomers are 8-amino-2-quinolinecarboxylic acid “Q” and 6-aminomethyl-2-pyridinecarboxylic acid “P” shown in Chart 1. Oligomers  $Q_n$  belong to the family of aromatic amide foldamers<sup>1a,c,f,g</sup> and have been shown to adopt exceptionally stable and rigid helical conformations in which adjacent amide and quinoline units lie almost coplanar to each other due to conjugation, local electrostatic repulsions, and hydrogen bonding.<sup>15,16</sup> For example the Gibbs activation energy of helix handedness inversion of  $Q_n$  reaches values over 100 kJ.mol<sup>-1</sup> for  $n \geq 8$ , thereby allowing the chromatographic separation of *P* and *M* enantiomeric conformers.<sup>15c</sup> In contrast, the methylene moiety of **P** monomers introduces rotational freedom that results in a high flexibility within a sequence, to the extent that  $P_n$  oligomers show no sign of folding.<sup>14</sup> Additionally the methylene

- (2) (a) Delsuc, N.; Léger, J.-M.; Massip, S.; Huc, I. *Angew. Chem., Int. Ed.* **2007**, *46*, 214–217. (b) Maurizot, V.; Dolain, C.; Leydet, Y.; Léger, J.-M.; Guionneau, P.; Huc, I. *J. Am. Chem. Soc.* **2004**, *126*, 10049–10052. (c) Delsuc, N.; Hutin, M.; Campbell, V. E.; Kauffmann, B.; Nitschke, J. R.; Huc, I. *Chem.–Eur. J.* **2008**, *14*, 7140–7143. (d) Daniels, D. S.; Petersson, E. J.; Qiu, J. X.; Schepartz, A. *J. Am. Chem. Soc.* **2007**, *129*, 1532–1533. (e) Horne, W. S.; Price, J. L.; Keck, J. L.; Gellman, S. H. *J. Am. Chem. Soc.* **2007**, *129*, 4178–4180. (f) Price, J. L.; Horne, W. S.; Gellman, S. H. *J. Am. Chem. Soc.* **2007**, *129*, 6376–6377. (g) Khakshoor, O.; Demeler, B.; Nowick, J. S. *J. Am. Chem. Soc.* **2007**, *129*, 5558–5569. (h) Petersson, E. J.; Schepartz, A. *J. Am. Chem. Soc.* **2008**, *130*, 821–823. (i) Qiu, J. X.; Petersson, E. J.; Matthews, E. E.; Schepartz, A. *J. Am. Chem. Soc.* **2006**, *128*, 11338–11339. (j) Sharma, G. V. M.; Subash, V.; Narsimulu, K.; Ravi Sankar, A.; Kunwar, A. C. *Angew. Chem., Int. Ed.* **2006**, *45*, 8207–8210. (k) Burkoth, T. S.; Beausoleil, E.; Kaur, S.; Tang, D.; Cohen, F. E.; Zuckermann, R. N. *Chem. Biol.* **2002**, *9*, 647–654. (l) Lee, B.-C.; Zuckermann, R. N.; Dill, K. A. *J. Am. Chem. Soc.* **2005**, *127*, 10999–11009. (m) Hu, H.-Y.; Xiang, J.-F.; Yang, Y.; Chen, C.-F. *Org. Lett.* **2008**, *10*, 68–72.
- (3) (a) Ramirez-Alvarado, M.; Blanco, F. J.; Serrano, L. *Nat. Struct. Biol.* **1996**, *7*, 604–612. (b) de Alba, E.; Jimenez, M. A.; Rico, M. *J. Am. Chem. Soc.* **1997**, *119*, 175–183. (c) Maynard, A. J.; Searle, M. S. *Chem. Commun.* **1997**, 1297–1298. (d) Maynard, A. J.; Sharman, G. J.; Searle, M. S. *J. Am. Chem. Soc.* **1998**, *120*, 1996–2007. (e) Griffiths-Jones, S. R.; Sharman, G. J.; Maynard, A. J.; Searle, M. S. *J. Mol. Biol.* **1998**, *284*, 1597–1609. (f) Stanger, H. E.; Gellman, S. H. *J. Am. Chem. Soc.* **1998**, *120*, 4236–4237. (g) Espinosa, J. F.; Syud, F. A.; Gellman, S. H. *Protein Sci.* **2002**, *11*, 1492–1505.
- (4) (a) Cochran, A. G.; Skelton, N. J.; Starovasnik, M. A. *Proc. Natl. Acad. Sci. U.S.A.* **2001**, *98*, 5578–5583. (b) Butterfield, S. M.; Waters, M. L. *J. Am. Chem. Soc.* **2003**, *125*, 9580–9581. (c) Mahalakshmi, R.; Raghobama, S.; Balaran, P. *J. Am. Chem. Soc.* **2006**, *128*, 1125–1138. (d) Ramagopal, U. A.; Ramakumar, S.; Sahal, D.; Chauhan, V. S. *Proc. Natl. Acad. Sci. U.S.A.* **2001**, *98*, 870–874. (e) Rudresh; Ramakumar, S.; Ramagopal, U. A.; Inai, Y.; Goel, S.; Sahal, D.; Chauhan, V. S. *Structure* **2004**, *12*, 389–396.
- (5) (a) Neidle, S. *Principles of Nucleic Acid Structure*; Academic Press: London, 2008. (b) *Quadruplex Nucleic Acids*; Neidle, S., Balasubramanian, S., Eds.; RSC Publishing, U.K., 2006.
- (6) (a) Haldar, D.; Jiang, H.; Léger, J.-M.; Huc, I. *Angew. Chem., Int. Ed.* **2006**, *45*, 5483–5486. (b) Haldar, D.; Jiang, H.; Léger, J.-M.; Huc, I. *Tetrahedron* **2007**, *63*, 6322–6330.
- (7) (a) Horne, W. S.; Gellman, S. H. *Acc. Chem. Res.* **2008**, *41*, 1399–1408, and references therein. (b) Choi, S. H.; Guzei, I. A.; Spencer, L. C.; Gellman, S. H. *J. Am. Chem. Soc.* **2008**, *130*, 6544–6550. (c) Sharma, G. V. M.; Jadhav, V. B.; Ramakrishna, K. V. S.; Jayaprakash, P.; Narsimulu, K.; Subash, V.; Kunwar, A. C. *J. Am. Chem. Soc.* **2006**, *128*, 14657–14668. (d) Seebach, D.; Jaun, B.; Sebesta, R.; Mathad, R. I.; Flögel, O.; Limbach, M.; Sellner, H.; Cottens, S. *Helv. Chim. Acta* **2006**, *89*, 1801–1825. (e) Jagadeesh, B.; Prabhakar, A.; Sarma, G. D.; Chandrasekhar, S.; Chandrashekar, G.; Reddy, M. S.; Jagannadh, B. *Chem. Commun.* **2007**, 371–373. (f) Baldauf, C.; Günther, R.; Hofmann, H. *J. Biopolymers* **2006**, *84*, 408–413. (g) Chatterjee, S.; Vasudev, P. G.; Ananda, K.; Raghobama, S.; Shamala, N.; Balaran, P. *J. Org. Chem.* **2008**, *73*, 6595–6606. (h) Vasudev, P. G.; Ananda, K.; Chatterjee, S.; Aravinda, S.; Shamala, N.; Balaran, P. *J. Am. Chem. Soc.* **2007**, *129*, 4039–4048. (i) Choi, S. H.; Guzei, I. A.; Spencer, L. C.; Gellman, S. H. *J. Am. Chem. Soc.* **2009**, *131*, 2917–2924.
- (8) (a) Garric, J.; Léger, J.-M.; Huc, I. *Angew. Chem., Int. Ed.* **2005**, *44*, 1954–1958. (b) Bao, C.; Kauffmann, B.; Gan, Q.; Srinivas, K.; Jiang, H.; Huc, I. *Angew. Chem., Int. Ed.* **2008**, *47*, 4153–4156.
- (9) Gong, B.; et al. *Proc. Natl. Acad. Sci. U.S.A.* **2002**, *99*, 11583–11588.
- (10) (a) Gabriel, G. J.; Sorey, S.; Iverson, B. L. *J. Am. Chem. Soc.* **2005**, *127*, 2637–2640. (b) Ghosh, S.; Ramakrishnan, S. *Angew. Chem., Int. Ed.* **2004**, *43*, 3264–3268. (c) Zhang, W.; Horoszewski, D.; Decatur, J.; Nuckolls, C. *J. Am. Chem. Soc.* **2003**, *125*, 4870–4873. (d) Gabriel, G. J.; Iverson, B. L. *J. Am. Chem. Soc.* **2002**, *124*, 15174–15175. (e) Lokey, R. S.; Iverson, B. L. *Nature* **1995**, *375*, 303–305.
- (11) (a) Brüggemann, J.; Bitter, S.; Müller, S.; Müller, W. M.; Müller, U.; Maier, N. M.; Lindner, W.; Vögtle, F. *Angew. Chem., Int. Ed.* **2006**, *46*, 254–259. (b) Feigel, M.; Ladberg, R.; Engels, S.; Herbst-Hirmer, R.; Fröhlich, R. *Angew. Chem., Int. Ed.* **2006**, *45*, 5698–5702. (c) Boehmer, A.; Brüggemann, J.; Kaufmann, A.; Yoneva, A.; Mueller, S.; Mueller, W. M.; Mueller, U.; Vergeer, F. W.; Chi, L.; De Cola, L.; Fuchs, H.; Chen, X.; Kubota, T.; Okamoto, Y.; Vögtle, F. *Eur. J. Org. Chem.* **2007**, *1*, 45–52.
- (12) (a) Raynal, N.; Averlant-Petit, M.-C.; Bergé, G.; Didierjean, C.; Marraud, M.; Duru, D.; Martinez, J.; Amblard, M. *Tetrahedron Lett.* **2007**, *48*, 1787–1790. (b) Baruah, P. K.; Sreedevi, N. K.; Gonnade, R.; Ravindranathan, S.; Damodaran, K.; Hofmann, H.-J.; Sanjayan, G. *J. J. Org. Chem.* **2007**, *72*, 636–639. (c) Akazome, M.; Ishii, Y.; Nireki, T.; Ogura, K. *Tetrahedron Lett.* **2008**, *49*, 4430–4433. (d) Prabhakaran, P.; Kale, S. S.; Puranik, V. G.; Rajamohan, P. R.; Chetina, O.; Howard, J. A. K.; Hofmann, H.-J.; Sanjayan, G. *J. J. Am. Chem. Soc.* **2008**, *130*, 17743–17754. (e) Kendhale, A. M.; Gonnade, R.; Rajamohan, P. R.; Hofmann, H. J.; Sanjayan, G. *J. Chem. Commun.* **2008**, 2541–2543. (f) Srinivas, D.; Gonnade, R.; Ravindranathan, S.; Sanjayan, G. *J. J. Org. Chem.* **2007**, *72*, 7022–7025.
- (13) Hunter, C. A.; Spitaleri, A.; Tomas, S. *Chem. Commun.* **2005**, 3691–3693.
- (14) Delsuc, N.; Godde, F.; Kauffmann, B.; Léger, J.-M.; Huc, I. *J. Am. Chem. Soc.* **2007**, *129*, 11348–11349.
- (15) (a) Jiang, H.; Léger, J.-M.; Huc, I. *J. Am. Chem. Soc.* **2003**, *125*, 3448–3449. (b) Dolain, C.; Grélard, A.; Laguerre, M.; Jiang, H.; Maurizot, V.; Huc, I. *Chem.–Eur. J.* **2005**, *11*, 6135–6144. (c) Delsuc, N.; Kawanami, T.; Lefeuvre, J.; Shundo, A.; Ihara, H.; Takafuji, M.; Huc, I. *ChemPhysChem* **2008**, *9*, 1882–1890.
- (16) A dimer is flat; longer oligomers have a helical shape that imposes ca. 10° twists at the aryl-amide linkages. See ref 15.

Scheme 1. Synthesis of  $P_nQ_4$  and  $PQ_4P_nQ_4$  Oligomers<sup>a</sup>

<sup>a</sup> Conditions: (a) DCM, DIEA RT, 12 h, yield 57%; (b) TFA (12 equiv.), RT, 6 h, quantitative; (c) Boc-P-OH (1 equiv.), HBTU (1.5 equiv.), HOBT (1 equiv.), DMF, DIEA (5 equiv.), N<sub>2</sub>, 0.5 h RT, then add H-P<sub>n</sub>Q<sub>4</sub>-OMe (1 equiv.), DMF, RT, 16 h, yield 91% (2), 93% (3), 82% (4), 75% (5); (d) Boc-PQ<sub>4</sub>-OH (1 equiv.), HBTU (1.5 equiv.), HOBT (1 equiv.), DMF, DIEA (5 equiv.), N<sub>2</sub>, 0.5 h RT, then add H-P<sub>n</sub>Q<sub>4</sub>-OMe (1 equiv.), DMF, RT, 16 h, yield 80% (6), 82% (7), 79% (8), 71% (9).

moiety preferentially sets the pyridine and amide units at a  $\sim 90^\circ$  angle. (PQ)<sub>n</sub> sequences can accommodate this preference upon adopting the herringbone helix referred to above in which contiguous PQ dimers lie perpendicular to each other.<sup>14</sup>

We had indeed designed monomer **P** to bring about some flexibility as compared to **Q** but not to the extent eventually observed. Also included in the initial design was the following: (i) the assumption that **P** monomers should impart a curvature similar to that of **Q** because they comprise the same sequence of atoms at the inner rim, both are  $\delta$ -peptides, and would thus be compatible with the canonical helically folding motif of **Q<sub>n</sub>** oligomers and (ii) the assumption that the aminomethyl moiety would make sequence assembly much easier and give access to very long oligomers thanks to the higher reactivity of aliphatic amines with respect to aminoquinolines. As shown in the following, both of these features proved to be true.

We report here that the stepwise synthesis of hybrid sequences of **P** and **Q** units can be efficiently carried out up to at least 40 monomers, which represent a molecular weight of ca. 9 kDa. We also find that multiple adjacent or nonadjacent **P** units adopt a canonical helical conformation identical to that of **Q** provided a sufficient number of **Q** monomers template their folding. On a more fundamental ground, this study brought us into setting objective experimental criteria to define whether a structure is folded or not, taking into account the potential dynamics of structures.

## Results and Discussion

**Folding Propensity of P<sub>n</sub>Q<sub>4</sub> Oligomers.** Knowing that **P<sub>n</sub>** sequences are apparently too flexible to fold into a stable structure and that **P** monomers anyhow tend to promote 90° kinks, we explored whether a tetrameric **Q<sub>4</sub>** sequence at the C-terminus of a strand would have any effect on the conformation of several **P** units. The synthesis of Boc-P<sub>n</sub>Q<sub>4</sub>-OMe oligomers with  $n = 1-5$  is shown in Scheme 1. Starting from a quinoline tetramer which can be prepared on a multigram scale,<sup>17</sup> the first **P**<sup>18</sup> monomer is introduced as an acid chloride to react with the terminal aromatic amine, whereas subsequent

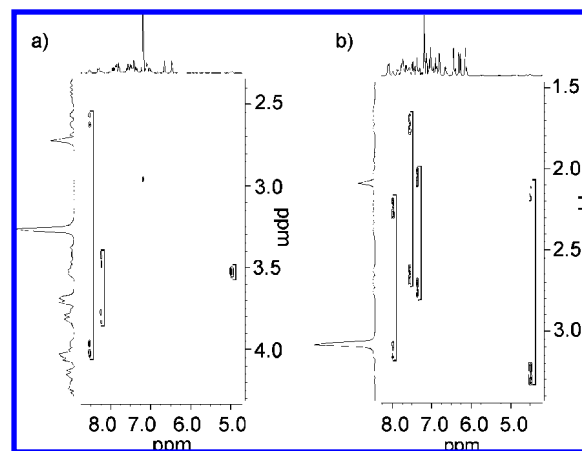


**Figure 1.** Representative examples of 2D COSY NMR spectra in CDCl<sub>3</sub> showing NH-CH<sub>2</sub> scalar couplings: (a) Boc-P<sub>3</sub>Q<sub>4</sub> (3); (b) Boc-PQ<sub>4</sub>P<sub>3</sub>Q<sub>4</sub>-OMe (8).

**Table 1.** Extent of the Diastereotopicity of the Main Chain Methylene Protons of Boc-P<sub>n</sub>Q<sub>4</sub>-OMe and Boc-PQ<sub>4</sub>P<sub>n</sub>Q<sub>4</sub>-OMe Oligomers As Measured by <sup>1</sup>H 2D COSY NMR

entry	$\Delta\delta$ (ppm)
Boc-PQ <sub>4</sub> -OMe	1.25 <sup>a</sup>
Boc-P <sub>2</sub> Q <sub>4</sub> -OMe	1.00, 0.20 <sup>a</sup>
Boc-P <sub>3</sub> Q <sub>4</sub> -OMe	1.40, 0.35, 0 <sup>a</sup>
Boc-P <sub>4</sub> Q <sub>4</sub> -OMe	1.00, 0.70, 0.25, 0 <sup>a</sup>
Boc-PQ <sub>4</sub> PQ <sub>4</sub> -OMe	1.00, 1.20 <sup>a</sup>
Boc-PQ <sub>4</sub> P <sub>2</sub> Q <sub>4</sub> -OMe	0.20, 1.00, 1.10 <sup>a</sup>
Boc-PQ <sub>4</sub> P <sub>3</sub> Q <sub>4</sub> -OMe	0.90, 0.95, 0.65, 1.10 <sup>a</sup>
Boc-PQ <sub>4</sub> P <sub>5</sub> Q <sub>4</sub> -OMe	1.05, 1.25, 0.85, 0.75, 0.60, 1.15 <sup>a</sup>

<sup>a</sup> Terminal carbamate unit.

**P** units are introduced via a simple HBTU/HOBT activation after deprotection of the Boc on the terminal aliphatic amines using TFA.

The <sup>1</sup>H NMR spectra of **1-5** in CDCl<sub>3</sub> are sharp (see the Supporting Information) and exhibit features typical of the helical folding of the **Q<sub>4</sub>** segment: spreading of amide and aromatic resonances over a wide chemical shift range; deshielding of the aromatic amide protons because of their involvement in intramolecular H-bonding; shielding of the terminal methyl ester due to ring current effects; and diastereotopic motifs of the CH<sub>2</sub> signals of the isobutoxy side chains of the **Q** units. However, the spectra did not provide information about the folded or nonfolded state of the **P<sub>n</sub>** segment. Chemical shift values of signals assigned to protons of **Q<sub>4</sub>** (e.g., amide NH, aromatic CH, or the terminal methyl ester) or to **P<sub>n</sub>** (e.g., the terminal Boc-NH) do not vary in any meaningful way upon adding **P** monomers.<sup>19</sup> We then devised that an expected indication of the folding of the **P<sub>n</sub>** segment onto the **Q<sub>4</sub>** helical segment would be substantially different chemical shift values of the two main chain benzylic methylene protons of each **P** monomer which become diastereotopic in the vicinity of a helix. COSY <sup>1</sup>H NMR spectra were recorded to test this hypothesis (Figure 1a). Scalar couplings between each aliphatic amide (or carbamate) NH and the adjacent CH<sub>2</sub> protons were free from any overlap and allowed to unambiguously assess chemical shift values (see Table 1). The signals of the CH<sub>2</sub> protons were found in the 2.5–4 ppm range. These values are to be compared to

(17) Jiang, H.; Léger, J.-M.; Dolain, C.; Guionneau, P.; Huc, I. *Tetrahedron* **2003**, *59*, 8365–8374.

(18) The synthesis of **P** is reported in the supporting information. Note that this **P** unit differs from the monomer described in ref 14 in that it does not have an isobutoxy substituent in position 4.

(19) For an account on the chain-length dependence test, see: (a) Stone, M. T.; Heemstra, J. M.; Moore, J. S. *Acc. Chem. Res.* **2006**, *39*, 11–20.

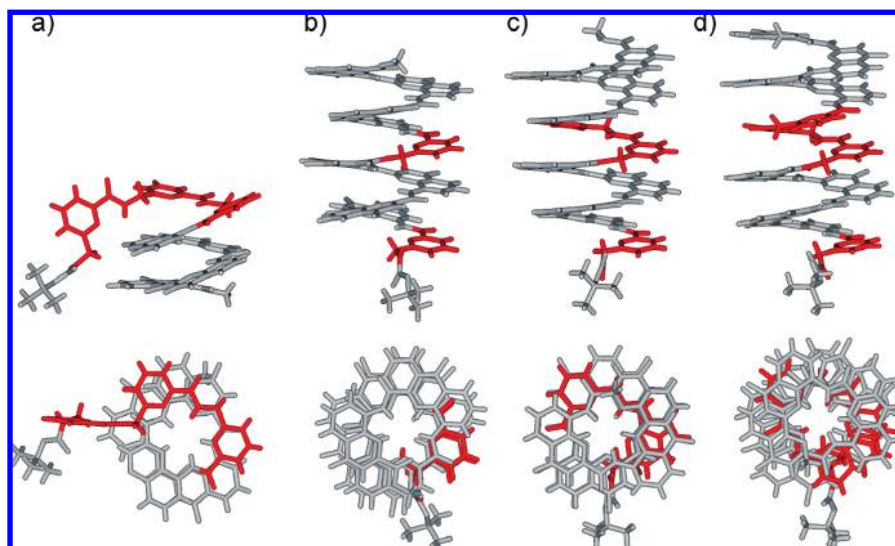


**Figure 2.** Side views (top) and top views (bottom) of the crystal structures of **3** (a), **6** (b), **7** (c), and **8** (d). Isobutyl side chains and included solvent molecules have been omitted for clarity. Quinoline units are shown in gray and pyridine units are shown in red.

4.5 ppm found for monomeric **P**, and thus indicate substantial ring current effects from the aromatic backbone. Moreover the extent of diastereotopicity ( $\Delta\delta$ ) between these protons varies greatly as the length of the  $P_n$  segment increases. Thus, the chemical shift difference at the carbamate terminus of Boc-**PQ**<sub>4</sub>-OMe is  $\Delta\delta = 1.26$  ppm indicating a strong effect of the helical environment. Upon increasing chain length, a couple  $\Delta\delta$  values remain high (Table 1), which we assign to the units closest to the **Q**<sub>4</sub> segment, but other values quickly drop down for the third most remote monomer and further, eventually reaching zero (no diastereotopicity).

The solution data were corroborated by the structure in the solid state of Boc-**P**<sub>3</sub>**Q**<sub>4</sub>-OMe (Figure 2a). This structure shows that the two **P** units closest to the **Q**<sub>4</sub> segment extend the helical motif of the quinolines. The terminal **P** unit, however, hangs out and lies in a plane parallel to the helix axis due to a rotation about a methylene moiety. Though this structure probably simply represents a snapshot of many conformations available to  $P_n$  segments, it is illustrative of the flexibility of this backbone and supports the conclusion that long  $P_n$  sequences do not adopt a stable helical conformation even when attached to a helical **Q**<sub>4</sub> segment.

**Folding Propensity of  $PQ_4P_nQ_4$  Oligomers.** In a second step, we evaluated the folding propensity of  $P_n$  segments inserted inbetween two stable helical **Q**<sub>4</sub> segments. Thanks to the aliphatic amines of **P**, the synthesis of Boc-**PQ**<sub>4</sub>**PQ**<sub>4</sub>-OMe **6** proceeded smoothly from two **PQ**<sub>4</sub> precursors using HBTU/HOBT activation (Scheme 1). Compounds **7–9** were prepared in a similar fashion. Their <sup>1</sup>H NMR spectra (Figure 3) all feature a single set of sharp signals. Since all Boc-**PQ**<sub>4</sub>**P**<sub>*n*</sub>**Q**<sub>4</sub>-OMe oligomers possess two quinoline helical segments, they may in principle give rise to various diastereomeric conformers in which each **Q**<sub>4</sub> segment has either a *P* or *M* handedness.<sup>20</sup> Interconversion between these diastereomers is expected to be slow on the NMR time scale since helical handedness inversion of a single **PQ**<sub>4</sub> segment is slow (as evidenced by the diastereotopic patterns of the *CH*<sub>2</sub> signals of isobutoxy chains). The presence of only one set of signals for all these compounds thus suggests

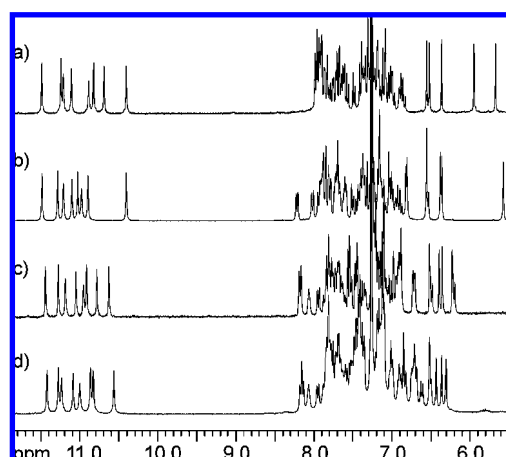


**Figure 3.** Part of the 300 MHz <sup>1</sup>H NMR of Boc-**PQ**<sub>4</sub>**P**<sub>*n*</sub>**Q**<sub>4</sub>-OMe in CDCl<sub>3</sub> at 25 °C showing aryl and amide resonances: (a) **6**, *n* = 1; (b) **7**, *n* = 2; (c) **8**, *n* = 3; and (d) **9**, *n* = 5.

that it corresponds to only one diastereomeric conformer in which the relative handedness of the **Q**<sub>4</sub> segments is strictly defined.<sup>21</sup>

Three of these compounds were crystallized and their structures in the solid state solved by X-ray crystallography. As shown in Figure 2, all **P** units involved in these structures adopt the helically folded conformation of the **Q**<sub>4</sub> segments; only the terminal Boc groups hang away from the helix backbone. In the case of Boc-**PQ**<sub>4</sub>**P**<sub>3</sub>**Q**<sub>4</sub>-OMe **8**, the three central **P** monomers span over one helical turn. Their contribution to helix curvature (number of units per turn) and to vertical rise (helical pitch) very closely approaches that of **Q** monomers. These structures thus validate our initial design that **P** and **Q** monomers could be combined in the same helical scheme, but it appears that a requirement for this is that  $P_n$  segments be flanked by **Q**<sub>4</sub> segments at both their extremities. Interestingly, the terminal Boc group is twisted away from the helix in each

(21) Though unlikely, the possibility that diastereomeric conformers would have rigorously identical NMR spectra cannot be ruled out on the basis of NMR measurements but was excluded based on chiral HPLC data.

(20) Dolain, C.; Léger, J.-M.; Delsuc, N.; Gornitzka, H.; Huc, I. *Proc. Natl. Acad. Sci. U.S.A.* **2005**, *102*, 16146–16151.

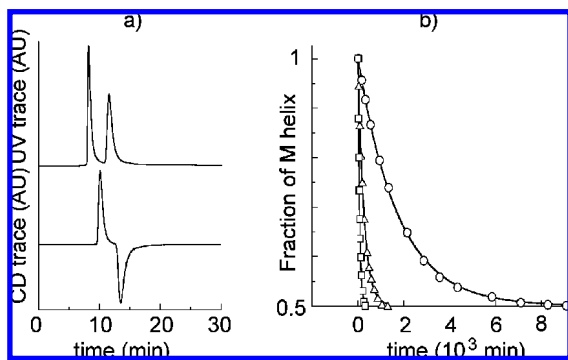


**Figure 4.** (a) Chromatogram of **8** on a Chiralpack IA column recorded at a column temperature of  $-5^{\circ}\text{C}$  eluting with n-hexane/chloroform (75:25, *v/v*) at  $0.5\text{ mL min}^{-1}$ . The CD curve is recorded at 385 nm and the UV curve at 350 nm; (b) Time courses of the racemization of the *M* helix at  $0^{\circ}\text{C}$  after its isolation, as monitored by chiral HPLC for **6** (○), **7** (Δ), and **8** (□).

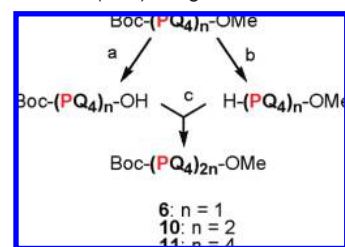
**Table 2.** Racemization Kinetic Data of **6**, **7**, **8**, and **10**

entry	<i>T</i> ( $^{\circ}\text{C}$ )	$k_{\text{rac}}$ ( $\text{s}^{-1}$ )	$t_{1/2}$ (h)	$\Delta G^{\ddagger}$ ( $\text{kJ mol}^{-1}$ )
Boc- <b>PQ</b> <sub>4</sub> <b>PQ</b> <sub>4</sub> -OMe	0	$4.8 \times 10^{-6}$	20	94
	10	$2.0 \times 10^{-5}$	4.9	95
	30	$2.8 \times 10^{-4}$	0.34	95
Boc- <b>PQ</b> <sub>4</sub> <b>P</b> <sub>2</sub> <b>Q</b> <sub>4</sub> -OMe	0	$3.3 \times 10^{-5}$	3.0	90
	10	$1.2 \times 10^{-4}$	0.81	90
	30	$1.4 \times 10^{-3}$	0.07	91
Boc- <b>PQ</b> <sub>4</sub> <b>P</b> <sub>3</sub> <b>Q</b> <sub>4</sub> -OMe	0	$1.3 \times 10^{-4}$	0.76	87
	10	$4.0 \times 10^{-4}$	0.24	88
	30	$1.5 \times 10^{-3}$	0.06	91
Boc-( <b>PQ</b> <sub>4</sub> ) <sub>4</sub> -OMe	0	$3.6 \times 10^{-7}$	260	100
	10	$1.5 \times 10^{-6}$	65	101
	30	$3.4 \times 10^{-5}$	2.8	100

crystal structure. This illustrates the intrinsic preference of  $\text{CH}_2$  moieties to set the CONH and pyridine groups at a  $90^{\circ}$  angle. Presumably because of the bulkiness and nonaromatic nature of the tBu group, there is no energy gain to fold it back on the helix surface. One may speculate that terminal aromatic carbamates or amides would have a tendency to fold back on the helix surface reflecting their propensity to engage in aryl–aryl interactions.

COSY spectra were recorded in this series as well (Figure 1b). Signals of the main chain  $\text{CH}_2$  protons were found in the 1.5–3.5 ppm range, indicating stronger ring current effects than in Boc-**P**<sub>*n*</sub>**Q**<sub>4</sub>-OMe and, contrary to those oligomers diastereotopicity remains strong for all **P** units (Table 1), even for a **P**<sub>5</sub> segment spanning two helical turns. Given these indications of stable folding, we sought for quantitative information on helix stability and carried out chiral HPLC experiments. We found that the *M* and *P* helical conformers of **6**, **7**, and **8**, but not **9**, could all be separated on a chiral stationary phase. The example of **8** is shown in Figure 4a using conditions described for **Q**<sub>*n*</sub> oligomers.<sup>15c</sup> The chromatograms were consistent with the <sup>1</sup>H NMR spectra and showed no trace of other diastereomeric conformers. A small sample of the pure *M* helix of each compound was isolated and its slow racemization was monitored by HPLC at different temperatures. These data were fitted to a simple first-order kinetic model to yield apparent kinetic constants and half-lives of racemization. Using the Eyring equation, the Gibbs energies of activation were also extracted (Table 2). These energies correspond to the difference between the folded state and an unfolded intermediate between *M* and *P* helices, and thus may be considered as a direct measurement of helix stability.<sup>15c</sup>

**Scheme 2.** Synthesis of (**PQ**<sub>4</sub>)<sub>*n*</sub> Oligomers<sup>a</sup>



<sup>a</sup> Conditions: (a) NaOH, THF/MeOH (1:1 vol/vol),  $30^{\circ}\text{C}$ , 2 h, quantitative; (b) TFA (12 equiv.), RT, 6 h, quantitative; (c) Boc-(**PQ**<sub>4</sub>)<sub>*n*</sub>-OH (1 equiv.), HBTU (1.5 equiv.), HOBT (1 equiv.), DMF, DIEA (5 equiv.),  $\text{N}_2$ , 0.5 h RT, then add H-(**PQ**<sub>4</sub>)<sub>*n*</sub>OMe (1 equiv.), DMF, RT, 16 h, yield 80% (**6**), 75% (**10**), 55% (**11**).

The major trend that emerges from this kinetics study is that helical oligomers tend to racemize faster upon adding **P** monomers in the sequence. This trend is opposite to that observed for **Q**<sub>*n*</sub> oligomers for which rates of racemization decrease rapidly when *n* increases.<sup>15c</sup> It reflects the high backbone flexibility imparted by **P** monomers which, even though they fit in the helical scheme, overall destabilize the structure. This also explains why no chromatographic data could be recorded for the longest oligomer **9** (Boc-**PQ**<sub>4</sub>**P**<sub>5</sub>**Q**<sub>4</sub>-OMe). Its rate of helix handedness inversion is too fast to allow the chromatographic separation of *M* and *P* helical conformers, even though it remains slow on the NMR time scale.

These results call for a discussion about the definition of “folded” in the case of **P**<sub>*n*</sub> segments flanked by **Q**<sub>4</sub> segments. “Folding” normally refers to a state in which units remote along a backbone come into close proximity. However, the results above suggest that **P**<sub>*n*</sub> segments undergo strong dynamics in solution and are unlikely to remain in the conformation they have in the solid state. Yet, even though **P**<sub>*n*</sub> segments may exist as an ensemble of multiple conformations, these equilibrate rapidly and possess an average handedness that is the same as the two **Q**<sub>4</sub> segments at the extremities of the sequence. It is thus the handedness that characterizes the folded state of **P**<sub>*n*</sub> segments: it defines two distinct ensembles of opposite chirality that equilibrate slowly on the NMR time scale and even on the chromatographic time scale in some cases; other ensembles in which **P**<sub>*n*</sub> oligomers would be flanked by **Q**<sub>4</sub> segments of opposite handednesses are not populated.

**Folding Propensity of (PQ<sub>4</sub>)<sub>n</sub> Oligomers.** The results above allow one to conclude that **Q** monomers indeed template the folding of adjacent **P** units, but that the latter nevertheless bring about flexibility in the helical conformations. What about nonadjacent **P** monomers? How many of them can be incorporated without allowing local inversion centers of handedness to occur? The synthesis of sequences comprised of a large number of **PQ**<sub>4</sub> repeat motifs was undertaken to address these questions. The choice of a tetrameric **Q**<sub>4</sub> segment to separate **P** units was driven by several considerations: (1) on a practical ground, a quinoline tetramer is easily accessible via a convergent synthetic scheme ( $1 + 1 = 2$ ;  $2 + 2 = 4$ );<sup>17</sup> (2) **Q**<sub>*n*</sub> helices possess exactly five units per turn. Targeting **PQ**<sub>4</sub> as a repeat motif was thus expected to allow to accurately probe whether the curvature imparted by **P** units is equal to that of **Q** units;  $3^{\circ}$  assuming that **P** and **Q** monomers impart the same curvature, (**PQ**<sub>4</sub>)<sub>*n*</sub> helices were thus expected to possess distinct faces with linear arrays of side-chains which could constitute the basis of side-by-side (zipper-like) associations between helices.

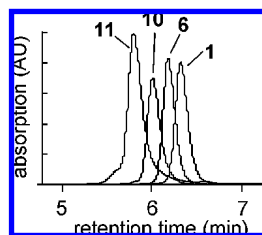


**Figure 5.** Overlay of the SEC traces of pentamer **1**, decamer **6**, 20mer **10**, and 40mer **11** on a TSK-GEL SUPER HM-M column. Conditions of separation compatible with the very low solubility of **11** were found using a  $\text{CHCl}_3$ /pyridine mixture (85:15 vol/vol) at 40 °C. Detection was carried out at 350 nm.

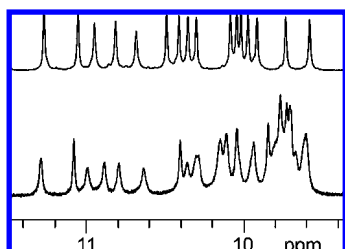


**Figure 6.** Part of the 700 MHz  $^1\text{H}$  NMR spectra of 20mer **10** (top) in  $\text{CDCl}_3$  and of 40mer **11** (bottom) in  $\text{CD}_2\text{Cl}_2$  showing aryl-CONH-aryl resonances.

As shown in Scheme 2, the segment doubling strategy that allowed decamer **6** from two pentamers to be produced was successfully applied to the synthesis of a 20mer from two decamers and even further to prepare a 40mer from two 20mers. At this stage, we experienced solubility problems for the first time in this chemistry and longer oligomers could not be prepared due to the very low solubility of the 40mer. However, one may predict that even longer oligomers may be prepared provided that **Q** monomers are functionalized with solubilizing groups more efficient than isobutoxy chains. It remains that the size of the 40mer (ca. 9 kDa) is unprecedented for a single chain synthetic helical oligomer prepared stepwise.<sup>22</sup> It is noteworthy that incorporating aliphatic amines compatible with the folding motifs alleviates the synthetic difficulties encountered in the stepwise preparation of long aromatic amide foldamers,<sup>9,15c,23</sup> or in their polymerization.<sup>24</sup> Only the living polymerization of tertiary aromatic polyamides approaches the level of control and product size that we achieved.<sup>25</sup>

A preliminary assessment of the size of these very long oligomers was performed by size exclusion chromatography (SEC) (Figure 5). The calculated molecular mass using a polystyrene standard was in all cases smaller than the actual mass, suggesting a compact conformation of the  $(\text{PQ}_4)_n$  oligomers: 1080 vs 1237 for pentamer **1**, 1630 vs 2337 for decamer **6**, 2780 vs 4528 for 20mer **10**, and 5080 vs 8916 for 40mer **11**. Despite their very large size and the repeat motif of their sequences, the  $^1\text{H}$  NMR spectra of both **10** and **11** feature a

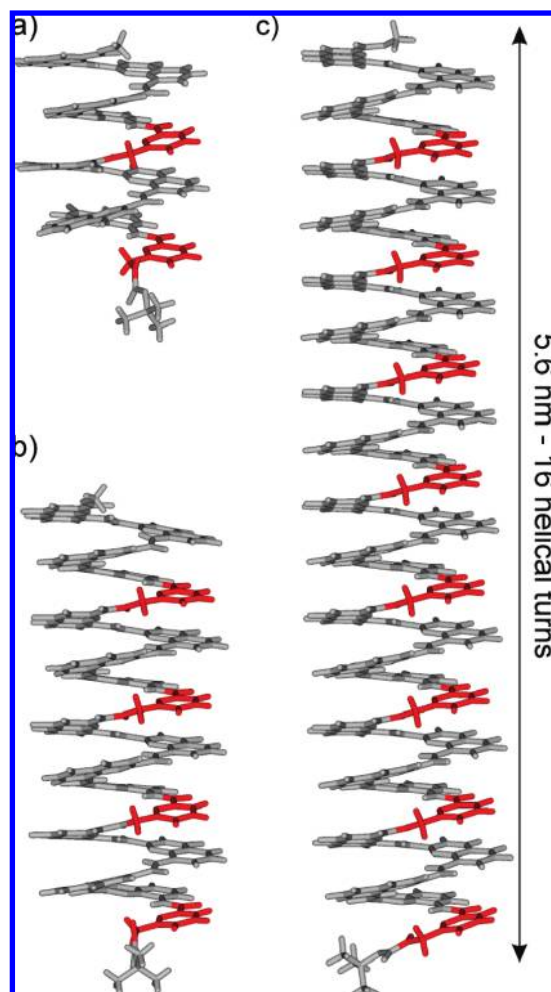


**Figure 7.** Side views of the crystal structures of **6** (a) and **10** (b) and of the energy minimized structure of **11** (c). Isobutyl side chains and included solvent molecules have been omitted for clarity. Quinoline units are shown in gray and pyridine units are shown in red.

single set of sharp signals spread over a wide chemical shift range with limited overlap (Figure 6). Thus, despite the multiple **P** monomers present in these sequences, no inversion of helix handedness occurs at these positions that would give rise to other diastereomeric forms. This was confirmed using chiral HPLC for 20mer **10** for which both helical enantiomers could be separated and their rate of racemization measured (Table 2). Kinetic data show that the helical conformation of 20mer **10** is more stable than that of decamer **6** by about  $5 \text{ kJ mol}^{-1}$ , which results in a half-life of helix handedness inversion at 0 °C of ca. 10 days for **10** versus 1 day for **6**. The effect of an additional two **P** units in the sequence of **10** as compared to **6** is largely compensated by the extra eight **Q** monomers. The same experiments could not be carried out with 40mer **11** because of its lack of solubility in the mobile phase required for efficient chiral chromatographic separation (*n*-hexane/chloroform, 75:25, *v/v*).

Further insights into the folding of Boc- $(\text{PQ}_4)_n$ -OMe oligomers were provided by the helical structure of 20mer **10** in the solid state (Figure 7). In addition to the structures of **6–8** (Figure 2), this structure further demonstrates the validity of our initial assumption that **P** and **Q** oligomers contribute equally to helix curvature and vertical rise. Indeed, the four **P** monomers of **10** are perfectly aligned in an array parallel to the helix axis, showing that the curvature of  $(\text{PQ}_4)_n$  is equal to five units per

(22) For a recent description of long ethylene glycol oligomers prepared stepwise, see: French, A. C.; Thomson, A. L.; Davis, B. G. *Angew. Chem., Int. Ed.* **2009**, *48*, 1248–1252.

(23) Zhang, A.; Ferguson, J. S.; Yamato, K.; Zheng, C.; Gong, B. *Org. Lett.* **2006**, *8*, 5117–5120.

(24) Jiang, H.; Léger, J.-M.; Guionneau, P.; Huc, I. *Org. Lett.* **2004**, *6*, 2985–2988.

(25) (a) Yokozawa, T.; Asai, T.; Sugi, R.; Ishigooka, S.; Hiraoka, S. *J. Am. Chem. Soc.* **2000**, *122*, 8313–8314. (b) Yokozawa, T.; Ogawa, M.; Sekino, A.; Sugi, R.; Yokoyama, A. *J. Am. Chem. Soc.* **2002**, *124*, 15158–15159.

two turns, as in  $Q_n$  oligomers. The methylene groups of the four  $P$  units are not thicker than aromatic groups and cause no bending of the rod-like helix. Attempts to crystallize 40mer **11** were hampered by the difficulty to obtain a sufficiently concentrated mother solution. Based on the structure of **10** a model of the helical conformation of **11** was calculated (Figure 7): it is expected to span 16 helical turns to reach of length of 5.6 nm.

In view of the strong ability of  $Q_4$  segments to template the helical folding of individual  $P$  monomers, one may wonder whether shorter  $Q_3$  or  $Q_2$  would work as well. This question can be answered with reasonable confidence in the light of the folding behavior of  $(PQ)_n$  oligomers that we described previously.<sup>14</sup> Indeed, the existence of a canonical helical conformation of  $(PQ)_4$  in solution was clearly recognized by NMR and molecular modeling, though at equilibrium with the unexpected noncanonical “herringbone” helix that accommodates the preference of the  $CH_2$  moieties to set the amide and pyridine groups at a  $90^\circ$  angle. There is thus no need of a long  $Q_n$  segment, not even one turn, to template the folding of  $P$  monomers into a canonical helix, but other folding modes may compete. One may thus expect  $Q$  units to template the folding of  $(PQ_2)_n$  or  $(PQ_3)_n$  into canonical helices that are more stable than the canonical helix of  $(PQ)_n$  but less stable than that of  $(PQ_4)_n$ , the overall helix stability being correlated to the ratio between  $P$  and  $Q$  units. It is difficult to completely rule out the existence of folds of  $(PQ_2)_n$  or  $(PQ_3)_n$  other than a canonical helix. However, considering that a simple  $PQ_2$  segment constitutes a rigid aromatic helix exceeding one turn, and in view of molecular models, other folding modes seem unlikely.

Our results also call for a discussion about the reasons behind the ability of  $Q_n$  segments to template the folding of  $P$  monomers and about the parameters that determine the nature and stability of the folded conformations of hybrid sequences. Oligomers comprised of  $P$  and  $Q$  consists of  $PQ_n$  ( $n = 0-2$  or more) aromatic amide segments which adopt a very stable crescent-like conformation in which all aromatic and amide groups lie coplanar ( $n < 2$ ) or almost coplanar when a helical conformation is reached ( $n \geq 2$ ). These large rigid segments are separated by a small and more flexible  $CH_2$  unit. Structure determinations show that  $CH_2$  units may adopt two distinct conformations, setting the adjacent amide and aryl moieties either at ca.  $90^\circ$ , or in a coplanar arrangement. The former appear to reflect the intrinsic conformational preference of the methylene moiety and has been observed in other benzylic monomers.<sup>20</sup> Examination of molecular models suggest that in this conformation, very limited, if any, aromatic stacking is allowed between (necessarily nonconsecutive) rigid segments, except for the herringbone helix of  $(PQ)_n$  oligomers. Furthermore, small deviations from this conformation generate steric clashes between the rigid helices. On the contrary, when aryl and amide groups adjacent to the  $CH_2$  moiety are coplanar (canonical helical folding), a bifurcated hydrogen bond forms

between the amide NH and the adjacent pyridine nitrogen atom, and extensive aromatic stacking is allowed between the helical segments, provided that they have the same helical handedness. Although aromatic stacking is presumably relatively weak in solvents like chloroform in which the above studies have been carried out, it appears to be an essential driving force to template the folding of  $P$  monomers in canonical helical conformations.

## Conclusion

Our study demonstrates that the introduction of aliphatic amines into aromatic oligoamides allows one to synthesize remarkably long rod-like folded helices using convergent schemes. The aliphatic units possess an overall poor folding propensity and conformation preferences that differ from those of the aromatic units. Nevertheless, aromatic units may impose their folding behavior to multiple contiguous or noncontiguous aliphatic units provided the former are in sufficient number. This majority rule is reminiscent of the “sergeant and soldier” principle proposed to explain the absolute handedness of some helical polymers comprised of monomers possessing opposite stereochemistry.<sup>26</sup> It also relates to the folding behavior of some peptides into sheets or helices that can be dictated by the preference of a small number of residues. In our hybrid sequences, the aliphatic units nevertheless make the helical structure less stable in that they allow helix handedness inversion to proceed faster. Upon adjusting the balance and sequence of aromatic and aliphatic residues, one can design helices of identical length and shape, but the stability of which may be tuned continuously over a wide range. The potential use of these unconventional molecular objects as components in nanomaterials and devices, for example as organizational scaffolds for photoinduced charge transfer,<sup>27</sup> is currently under investigation and will be reported in due course.

**Acknowledgment.** This work was supported by an ANR grant (Project No. NT05-3\_44880) and by the French Ministry of Research (ACI Nanoscience). We are very grateful to Christoph Mueller-Dieckmann for beamtime and technical assistance during data collection on ID29 beamline at ESRF (Grenoble).

**Supporting Information Available:** Synthetic schemes and procedures, characterization of new compounds, crystallographic information files, chromatographic data, and kinetic studies. This material is available free of charge via the Internet at <http://pubs.acs.org>.

JA9019758

- (26) (a) Green, M. M.; Reidy, M. P.; Johnson, R. J.; Darling, G.; O’Leary, D. J.; Willson, G. *J. Am. Chem. Soc.* **1989**, *111*, 6452–6454. (b) Green, M. M.; Park, J.-W.; Sato, T.; Teramoto, A.; Lifson, S.; Selinger, R. B. L.; Selinger, J. *Angew. Chem., Int. Ed.* **1999**, *38*, 3138–3154.
- (27) Wolfs, M.; Delsuc, N.; Veldman, D.; Van Anh, N.; Williams, R. M.; Meskers, S. C. J.; Janssen, R. A. J.; Huc, I.; Schenning, A. P. H. J. *J. Am. Chem. Soc.* **2009**, *131*, 4819–4829.